The Influence of Mechanical Surface Preparation Method, Adhesive Type, and Curing Temperature on the Bonding of Darwin Stringybark

William Leggate,[a,b,]* Robert L. McGavin,[b,c] Andrew Outhwaite,[b] Jack Dorries,[b] Rhianna Robinson,[b] Chandan Kumar,[b] Adam Faircloth,[b] and Mark Knackstedt [a]

Darwin stringybark (*Eucalyptus tetrodonta*) is one of Northern Australia's most important commercial forest resources. The wood exhibits desirable wood properties including high strength, natural durability, and visual appeal. The production of engineered wood products (EWPs) such as glulam from this resource represents a significant commercial opportunity for the timber industry in northern Australia. However, a major challenge to overcome is the achievement of satisfactory glue bond performance. This study evaluated the effects of different surface machining preparations, adhesive types, and curing temperatures on the bonding characteristics of Darwin stringybark. The pre-gluing surface machining method significantly influenced the timber wettability, roughness, permeability and tensile shear strength of adhesive bonds. Planing resulted in the lowest wettability, roughness, and permeability, while bonded planed samples produced the poorest tensile shear strength. Alternative surface machining methods including face milling and sanding post-planing were shown to significantly improve the timber wettability, roughness, and permeability, and also to increase the tensile shear strength of bonded samples. The resorcinol formaldehyde adhesive resulted in slightly improved tensile shear strength in most cases compared to the polyurethane adhesive. There was no significant improvement in tensile shear strength with the use of elevated temperature curing.

Keywords: Wood surface machining; Wood wettability; Wood permeability; Wood adhesion; Wood roughness; Eucalyptus tetrodonta; Darwin stringybark

Contact information: a: Research School of Physics and Engineering, The Australian National University, Canberra, ACT 0200, Australia; b: Queensland Department of Agriculture and Fisheries, Horticulture and Forestry Science, Salisbury Research Facility, 50 Evans Rd, Salisbury, Qld 4107, Australia; c: School of Civil Engineering, The University of Queensland, St. Lucia, Queensland, 4072, Australia;
** Corresponding author: william.leggate@daf.qld.gov.au*

INTRODUCTION

The demand for and use of engineered wood products (EWPs) continues to increase globally as consumers are increasingly favouring sustainable, low-embodied energy building products that are straighter, more stable, and uniform in size, exceed the performance capabilities of traditional timber products, are lighter in weight and have certified structural performance with reduced variability (Leggate 2018; Leggate *et al*. 2020a; Market Research Future 2020).

The northern Australian timber industry is well placed to service a niche market for EWPs with performance properties that are superior to products manufactured from common commercial timber species on the international market. Australia's native commercial timber species are dominated by the *Eucalyptus* and *Corymbia* species. Within these species, significant variation in wood properties exist; however, in general, Australia's native forest timbers have an international reputation for being superior in mechanical performance and in many cases, have good to excellent natural durability. For example, the wood density of most native hardwood commercial timber species in northern Australia far exceeds the wood density of plantation softwood species. All of Australia's plantation softwood species are regarded as non-durable; however, many of Australia's native commercial timber species are considered to be durable, including a high representation within the durability class 1 and 2 categories (on a 1-4 scale with class 1 being the most durable [Australian standard AS 5604 (2005)]). Using timbers that have high natural durability and superior mechanical properties to manufacture high performance EWPs enables high-value markets to be accessed with greatly reduced competition from other internationally produced timber products.

However, at the same time, the northern Australian hardwood timber industry is challenged, with decreasing average log diameter and diminishing overall log quality. While the forest and forest product industries strive to gain the most value from the available resources, some traditional timber products are becoming increasingly difficult to supply from lower quality and smaller diameter logs. For example, large dimension sawn timber posts and beams, which have been traditionally the target, profitable sawn product range for Australia's hardwood industry, are gradually less able to be produced. Instead, smaller board sizes are increasingly produced that more align with the available log resources. These products do not necessarily have the same market demand or attract the same premium prices. Indeed, the inability for the timber industry to reliably supply many of these traditional products has resulted in consumers seeking alternative products and in many cases, the timber industry are losing these once lucrative markets. To hold on to many traditional markets and to expand into new markets, EWPs that enable small section sawn boards to be glue-laminated together to form large dimension products such as post and beams are required.

While the durability and mechanical properties of northern Australian hardwoods are attractive for many lucrative markets, these same characteristics are also responsible for these timbers being very difficult to reliably glue. Several timber processors are currently trying to attain certification for glue-laminated products manufactured from spotted gum (*Corymbia citriodora*), Queensland's highest volume hardwood timber species. Despite many years of effort, a reliable adhesive protocol is yet to be developed. Darwin stringybark (*Eucalyptus tetrodonta)* has been identified as an alternative timber species to pursue for EWPs. With a similar or slightly better structural performance and natural durability rating, this species may be less problematic to glue due to the less greasy nature of the wood when compared to spotted gum; however, preliminary industry trials suggest that improved protocols are required. The development of gluing protocols that enables Darwin stringybark to be used in structural laminated post and beams presents a real opportunity for the northern Australian timber industry.

Surface machining is a standard international timber industry practice used to size and prepare the wood laminates prior to gluing (Leggate *et al*. 2020a). The most typical method used internationally is planing of the wood surface immediately before gluing (Knorz *et al*. 2015). Surface machining prior to adhesive application has been shown to improve wood adhesion by increasing the wettability of the wood surface and improving adhesive penetration and bonding by: 1) activating the wood surface through the removal of extractives (which have migrated to the surface) and contaminants (*e.g*. dust and dirt);

2) creating micro-cracks and exposing wood cell lumens; 3) rupturing the molecular bonds between wood components creating open bonds which increases the number of active sites for the adhesive polar groups to bond to; 4) creating a flat surface allowing for a close fit between the two wood adherents, and 5) increasing the number of mechanical interlocking sites for the adhesive to bond with the wood (Vick 1999; Sernek 2002; Aydin 2004; Vella 2020; Leggate *et al*. 2020a).

Limited international studies have compared the benefits for wood adhesion after different mechanical surface preparation methods such as planing, sanding, face milling, and more recently scarification or incising (Hernández and Cool 2008a,b; Kläusler *et al.* 2014; Knorz *et al.* 2015; Vella *et al*. 2019; Vella 2020; Leggate *et al.* 2020a,b). Wood face milling is not currently used commercially in Australia and has not yet been adequately tested on Australian timbers as a means to improve wood adhesion (Leggate *et al.* 2020b). However, face milling is reported in some studies to produce better results for wood adhesion compared to conventional planing due to the cutting action (perpendicular to the grain) generating lower cutting forces and consequently lower sub-surface damage of the wood structure compared to conventional planing (cutting direction parallel to the grain) (Santoni and Pizzo 2011; Kläusler *et al.* 2014; Knorz *et al.* 2015). The lower cutting forces result from the lower strength of the wood in the transverse direction (de Moura *et al*. 2010; Knorz *et al.* 2015). As a result, sub-surface cell damage which results in the formation of a mechanically weak boundary layer that causes poor bond performance and failure is likely to be reduced with face milling (De Moura *et al.* 2010; Kläusler *et al.* 2014).

Follrich *et al.* (2010) reported increased tensile strength of bonds with increased surface roughness, although the findings regarding the influence of roughness on bonding performance are not fully consistent (Kläusler *et al.* 2014) with excessive roughness sometimes resulting in decreased bond strength. This was particularly so, if it is associated with crushed and damaged cells becoming prevalent that can lead to a mechanically weak boundary layer and also impeded adhesive penetration (Knorz *et al.* 2015). Previous research by Leggate *et al*. (2020a,b) indicates that face milling and sanding post-planing can improve the wettability and the permeability of spotted gum timber and also improve the tensile shear strength of spotted gum glued wood joints.

Apart from surface machining, other priority research areas being targeted to improve the adhesion of Darwin stringybark and spotted gum include investigations into optimal adhesive types and curing conditions. Historically, the most common adhesives used in the manufacture of glulam have been resorcinol formaldehyde (RF) and phenol resorcinol formaldehyde (PRF) (Vella *et al.* 2019). However, polyurethane adhesives such as 1C-PUR are increasingly replacing RF and PRF because of many advantages including faster curing properties, lack of formaldehyde emissions and a single component system that is supplied ready to use (Lehringer and Gabriel 2014; Vella *et al.* 2019). One reason that there has been limited use of PUR adhesives for hardwoods in Australia has been because of concerns over their suitability with higher density timbers. They have been traditionally used with lower density timbers and not yet adequately tested with northern Australian high-density hardwood timbers. Most adhesives used for glulam production are also cured during pressing at ambient temperature curing conditions. However, heating during curing of RF adhesives is thought to improve adhesive penetration and also support complete curing of the adhesive within the target press time.

This study investigates the effect of various surface machining preparation methods, adhesive types and curing temperatures on the bonding of Darwin stringybark sawn timber. Its primary aim is to contribute to the development of optimal adhesion protocols for this species for glulam production.

EXPERIMENTAL

Wood Sample Preparation

Twenty seasoned boards (nominally 100 mm × 25 mm) of native forest sourced Darwin stringybark were randomly selected from commercial packs of milled timber destined for products such as flooring and decking. A 25 mm long cross section was removed from the middle of each board for moisture content determination using the oven-dry method in accordance with Australian and New Zealand standard AS/NZS 1080.1 (2012).

Each board was ripped and docked to provide twelve pieces free of sapwood and defects, with dimensions of 30 mm ×11 mm × 400 mm (W × T × L). These pieces were then conditioned in a constant environment chamber set at 20 °C and 65% relative humidity (RH) (12% equilibrium moisture content [EMC]). After conditioning, 180 samples were randomly allocated to three different mechanical surface machining preparations providing 60 samples per machining treatment (Table 1).

Table 1. Mechanical Surface Machining Preparations

Surface Machining Identifier	Surface Machining Method	Cutter Specifications	Feed, Cutter and Sanding Speeds
SM1	Face Milling (fast feed speed and slow cutter speed)	Type: Tungsten Carbide Pt No: Leucodur – HL 40 Dim: 14 x 14 x 2 mm 48 Cutters @ 520 mm diameter	Feed rate = 45 m/min, Cutter speed = 2100 rpm (57 m/s)
SM2	Planing	High Speed Steel Blade 40.5° Blade tip angle 120 mm Cutterblock diameter	Feed Rate: 8 m/min Cutter RPM: 4500 (28 m/s)
SM3	Sanding (40 grit) Post-Planing	Belt : KLINGSPOR PS 29 F Grit: Aluminium Oxide Backing: Paper diameter	Planed 8 m/min feed rate + Sanding using 40 grit belt removing 0.3 mm Belt Speed = 18 m/min Feed rate = 3.5 m/min

Face milling was undertaken using a Rotoles 400 D-S single side rotary planer manufactured by Ledinek (Hoče, Slovenia). This face milling approach has the rotary head and cutters positioned parallel to the machining surface with the drive shaft positioned perpendicular to the board surface (Fig. 1a). The cutting direction with face milling is primarily perpendicular to the grain (Knorz *et al.* 2015; Leggate *et al.* 2020b). Conventional planing was undertaken using a SCM Group Mini Max Formula SPI thickness planer (Rimini, Italy). The conventional planer has the cutter head drive shaft positioned parallel to the board surface (Fig. 1b). The cutting direction with conventional planing is primarily parallel to the grain (Knorz *et al.* 2015; Leggate *et al.* 2020b). Sanding used a SCM Group SANDYA 16/S M2 135 wide belt sander (Rimini, Italy).

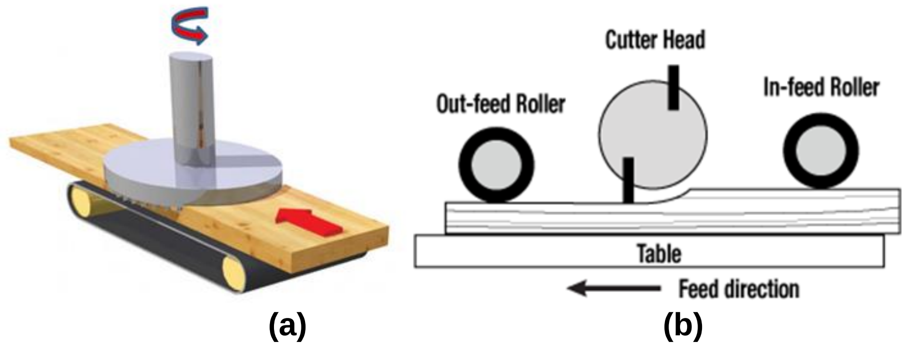

Fig. 1. Machining preparation method comparison between (a) Rotoles face milling approach (Ledinek 2020) and (b) Conventional planing approach (CCOHS 2020)

During each surface machining process described in Table 1, 1.5 mm was removed from the upper and lower timber surface to reduce the thickness from 11 mm to 8 mm. Test samples were then prepared to the final dimension for wettability and roughness tests (30 mm × 8 mm × 50 mm [W × T × L]), permeability tests (24 mm [diameter] × 8 mm [T]), and lap shear pieces (20 mm × 8 mm × 80 mm [W × T × L]). Lap shear pieces combine as pairs for the manufacture of lap shear samples.

Wettability

The wettability of wood refers to an adherend's ability to attract a liquid, such as an adhesive (Hovanec 2015). Adequate wetting of the surfaces of adherends is necessary to achieve a strong adhesive bond (Wellons 1980; River *et al.* 1991; Hovanec 2015; Leggate *et al.* 2020a). The wettability was determined by using the sessile drop method: by measuring the contact angle of a drop of pure water on the timber surface (Burch 2015; Leggate *et al.* 2020a). Testing followed the methodology adopted by Leggate *et al.* (2020a). Contact angle is the angle that the liquid forms with a solid, shown in Fig. 2 (Burch 2015; Leggate *et al.* 2020a). Since the tendency for a liquid to spread increases as contact angle decreases, the determination of contact angles is a useful inverse measure of wettability (Zisman 1964; Leggate *et al.* 2020a). In order to compare the change in timber wettability with time elapsed since surface machining, contact angles were measured at two time intervals: 0 minutes (therefore immediately after surface machining) and 15 minutes after surface preparation.

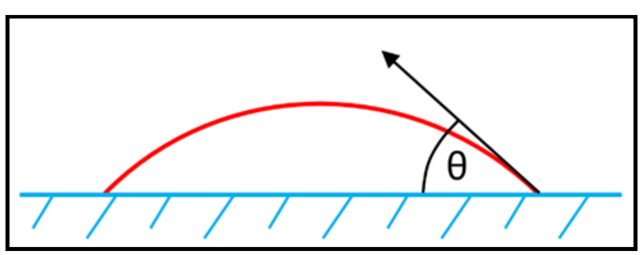

Fig. 2. Contact angle (θ) for a liquid droplet on a solid surface (Burch 2015)

An electronic pipette (Labco Electronic Pipettor, Labco Limited, Lampeter, Wales) was mounted on a stand so that the default position of the pipette tip was approximately 20 mm from the sample surface. The pipette could be moved vertically towards the sample surface to place a water droplet onto the sample surface but automatically retracted once manual control was released. A video camera (Samsung Galaxy A20, Samsung, Seoul, South Korea) was positioned approximately 10 mm in front of the sample and level with the timber surface. The camera was used to record the process of the droplet being applied and spreading on the sample surface. A clip-on macro lens (Apexel, APL-24XMH, Shenzen Apexel Technology Co. Ltd, Guangdong, China) was attached to the camera to provide adequate magnification of the droplet. The macro lens and camera combined provided approximately 50x magnification (21x from the macro lens and about 2.5x from the camera). The camera was securely mounted to prevent movement and vibration. A droplet of 1 µlitre water (HPLC-grade) was dispensed from the pipette per test. The pipette was manually repositioned towards the sample surface to aid dispensing and then immediately retracted once the droplet moved onto the sample surface. The process of the droplet dispensing and a minimum of ten seconds following were recorded by video.

For each sample, screenshots of the video were saved as images at specific times. The first image was taken once the pipette had applied the droplet on the surface (Fig. 3A), and then one image was taken per second for 10 seconds, providing a total of 11 contact angle images. These images were processed by the open-source software, ImageJ (IJ 1.46r) (U.S. National Institutes of Health, Maryland, USA) (Schneider *et al*. 2012) with the contact angle plugin (Lamour *et al.* 2010) (Fig. 3B). For each ImageJ measurement, two points were manually selected at the intersection of solid-liquid-air interfaces (marked by an arrow in Fig 3A) to define the baseline and four points along the drop profile. The ImageJ contact angle plugin then fitted the points with the sphere approximation or ellipse approximation and calculated the contact angle.

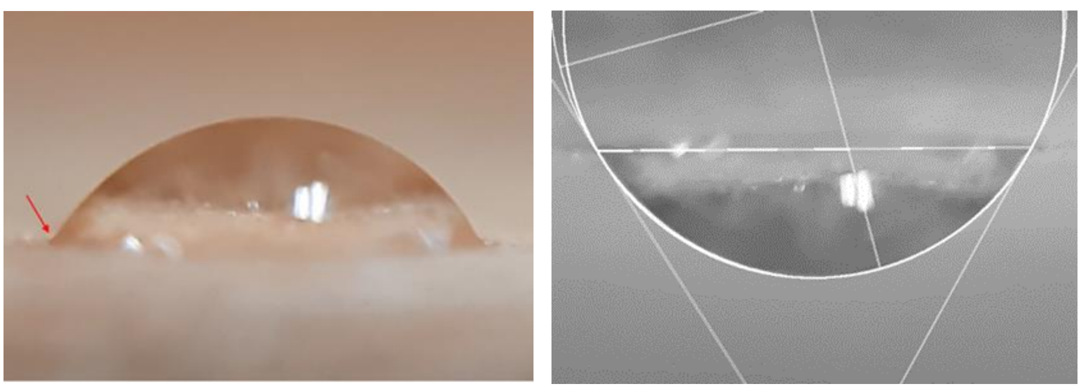

(a) **(b)**

Fig. 3. Water droplet in contact with timber surface. (a) A drop of water on timber surface. (b) Same drop as in (a) processed with the ImageJ software (note the image is inversed as part of the processing).

The change in contact angle over time was assessed using the method adopted by Burch (2015) and Leggate *et al.* (2020a), where a wetting model was developed to quantify the change in contact angle over time. The wetting model is shown in Eq. 1,

$$\theta = \frac{\theta_i \theta_e}{\theta_i + (\theta_e - \theta_i)\exp\left[K\left(\frac{\theta_e}{\theta_e - \theta_i}\right)t\right]} \quad (1)$$

where θ_i is the initial contact angle at time 0 sec, θ_e is the equilibrium contact angle (for our data, at the 10 second test time), t is time (seconds), and K is the constant intrinsic relative contact angle decrease rate (1/s). The *K*-value represents the rate at which a liquid spreads and penetrates across or into the wood substrate (Shi and Gardner 2001; Burch 2015; Leggate *et al*. 2020a). A high *K*-value represents a liquid that quickly spreads and/or penetrates into the wood surface, while a low *K*-value represents a liquid that slowly spreads and/or slowly penetrates into the wood surface. A *K*-value of zero represents no change between initial and equilibrium contact angles (Burch 2015). The nonlinear least square method was used to estimate the *K*-value of the nonlinear model using R studio (Baty *et al.* 2015; RStudio Team 2015). The contact angle values at time 0 s and at 10 s were assigned as initial (θ_i) and equilibrium (θ_e) contact angle, respectively. The initial value of *K* was assigned to 0.3 in the nls function. Contact angle and *K*-values were determined for sixty samples from each surface machining group.

Roughness

Surface roughness is the measurement of the small-scale variations in the height of a physical surface (Butler 2008). Surface roughness has been shown to have a major impact on the wettability, permeability, and bonding performance of wood (Hernández and Cool 2008a; Santoni and Pizzo 2011; Kläusler *et al.* 2014; Knorz *et al.* 2015; Qin *et al.* 2015; Jankowska *et al.* 2018; Leggate *et al.* 2020a,b). Surface roughness was measured using a Mitutoyo surface roughness meter (SJ-210, Mitutoyo America Corporation, Aurora, Illinois, USA). A single roughness profile was taken on the surface of 60 samples from each surface machining method. The traverse was completed perpendicular to the grain (Fig. 4) using the parameters outlined in Table 2. Each sample was secured to prevent any potential movement during the measurement process. The surface roughness meter calibration was confirmed every 20 measurements.

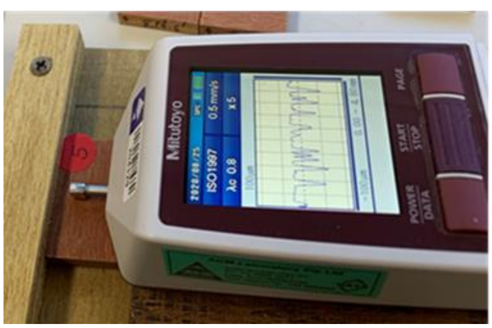

Fig. 4. Surface roughness assessments using the SJ-210 roughness meter

Table 2. Parameters Used for Surface Roughness Evaluation

Tracing length	100 µm
Tracing speed	0.5 mm/s
Cut-off length λc	0.8
Force	0.75 mN
Stylus tip radius	2 µm
Stylus tip angle	60°
Stylus tip material	Diamond
Standard	ISO 4287 (1997)
Filter	GAUSS

From the surface roughness meter, the R_a value was extracted. The R_a is described as the arithmetic mean of the absolute values of the evaluation profile deviations (Y_i) from the mean line. This method of calculating R_a was in accordance with ISO 4287 (1997) and is shown in Eq. 2,

$$R_a = \frac{1}{n}\sum_{i=1}^{n}|Y_i| \tag{2}$$

Permeability

Permeability is a measure of the ease with which liquids and gases flow through a porous substance under the influence of a pressure gradient (Comstock 1968; Tesoro 1973; Milota *et al*. 1994; Leggate *et al*. 2019, 2020a). The permeability of wood influences many of its important processing and utilization properties including gluing, but also drying, preservation, wood modification systems, pulping, finishing, and even durability (Fogg 1968; Tesoro 1973; Hansmann *et al.* 2002; Zimmer *et al*. 2014; Leggate *et al.* 2019, 2020a). Wood permeability is one of the main controlling factors influencing the depth of adhesive penetration (Burch 2015; Hovanec 2015; Kumar and Pizzi 2019).

Sixty permeability samples were prepared from each surface machining group. Samples for permeability tests were 24 mm in diameter and 8 mm in thickness (flow direction). Each sample was coated with epoxy resin on its lateral surface in order to direct gas movement in the radial direction in order to measure only radial gas permeability. Radial gas permeability measurements were undertaken using a Porolux 1000 Porometer (1B-FT GmbH, Berlin, Germany). Samples were subjected to pressurized, atmospheric air until pressure reached the target pressure of 4000 millibars. All permeability measurements were recorded in less than 45 min after surface machining. Permeability was calculated in accordance with Darcy's law as follows,

$$Q = K \cdot \frac{A}{L} \cdot \frac{1}{\eta}\, \Delta P \tag{3}$$

where $Q, K, A, L, \eta, \Delta P$ are the liquid or air volume flow rate ($m^3.s^{-1}$), permeability of wood (m^2), area perpendicular to the liquid flow (m^2), sample length in the direction of flow (m), dynamic viscosity of the liquid or air (Pa.s), and the pressure drop, respectively (Pa) (Kucerová 2012). Permeability was reported in millidarcy units (mD).

Lap Shear Sample Manufacture

Sixty lap shear samples were prepared for each of the three surface machining types following the principles of European Standard BS EN 205 (2016). Lap shear sample dimensions are shown in Fig. 5. The application of adhesive commenced within a maximum of 20 minutes from surface machining. The adhesive bonded overlap in the lap shear samples was 10 mm as per Fig. 5. Therefore, the resultant length of the bonded lap shear samples was 150 mm (Fig. 5). A one-component moisture-curing polyurethane (1C-PUR) adhesive (Jowat Jowapur 686.70) and a resorcinol formaldehyde (RF) (Hexion Sylvic R15 Resin and Hexion RP50 Paraformaldehyde Hardener mixed in a ratio of 4 parts resin to 1 part hardener) adhesive were both tested. These glue types are representative of typical glues targeted commercially in structural glulam production in Australia. In accordance with the technical data sheets for these adhesives, one third of the lap shears (20 pairs per surface machining treatment) had 1C-PUR applied at a spread rate of 250 grams per square metre (gsm) and the remaining lap shears (40 pairs per surface machining treatment) had RF adhesive applied at a spread rate of 350 gsm evenly spread over one side of the lap shear joint. Open assembly time was less than 30 seconds for both adhesives, and closed assembly time was 30 minutes for the RF adhesive samples and less than 5 minutes for the PUR adhesive samples.

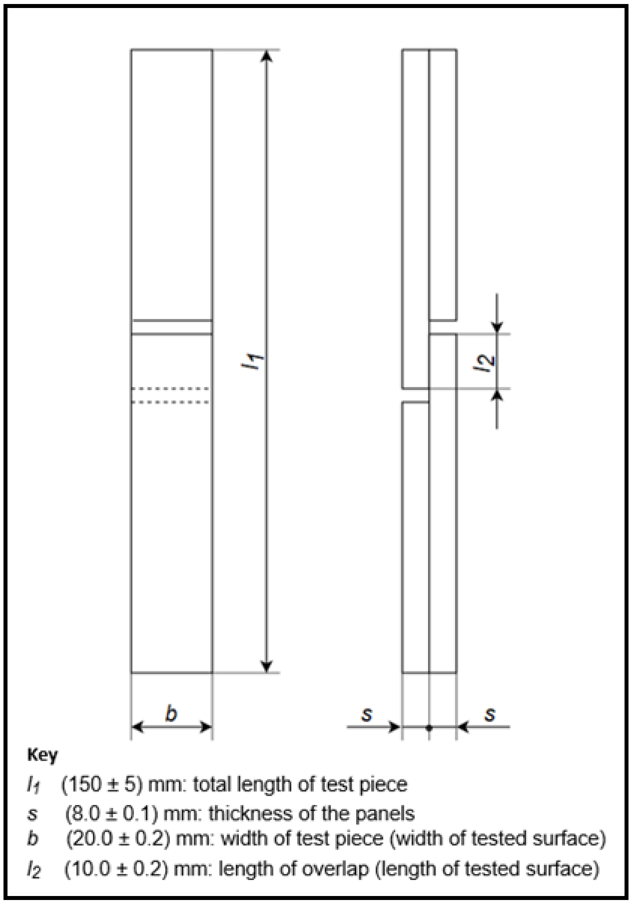

Fig. 5. Lap shear sample dimensions

The lap shear samples were pressed at 0.8 MPa for 1C-PUR samples and 1 MPa for the RF samples. The 1C-PUR lap shear samples remained under press pressure for a minimum of 180 minutes in ambient conditions, whereas one half (20 pairs) of the RF samples were pressed for a minimum of 14 h in ambient conditions. The remaining half of the RF samples (20 pairs) were pressed at 1 MPa at an elevated temperature of 65 °C for a minimum of 6 h. After pressing, all lap shear samples were then conditioned in a constant environment chamber set at 30 °C and 67% RH (12% EMC) for a minimum of 7 days before tensile shear strength testing.

Tensile Shear Strength Test Method

Tensile shear strength is a measure of the shear strength of an adhesive bond in which two members are bonded in a lap joint, then pulled at both ends until the joint fails in shear (Gooch 2011). The determination of the tensile shear strength of lap joints was undertaken in accordance with the BS EN 205 (2016) standard. Lap shear tensile testing was conducted using a Shimadzu AG-X Universal Testing Machine (AG-100X; Shimadzu Corporation, Kyoto, Japan) configured with a crosshead displacement rate of 1.5 mm/min. The data were processed using Trapezium X single cycle software (Shimadzu Corporation, Version 1.5.1, Kyoto, Japan). The lap shear samples had a minimum of 40 mm of each end clamped into the jaws of the testing rig before being loaded in tension until sample failure (Fig. 6). The maximum force applied to reach failure was recorded. The tensile shear strength, τ (MPa) was then calculated using Eq. (4),

$$\tau = \frac{F_{max}}{l_2 b} \tag{4}$$

where F_{max} is the applied maximum force (N), l_2 is the length of bonded test surface (mm), b is the width of bonded test surface (mm).

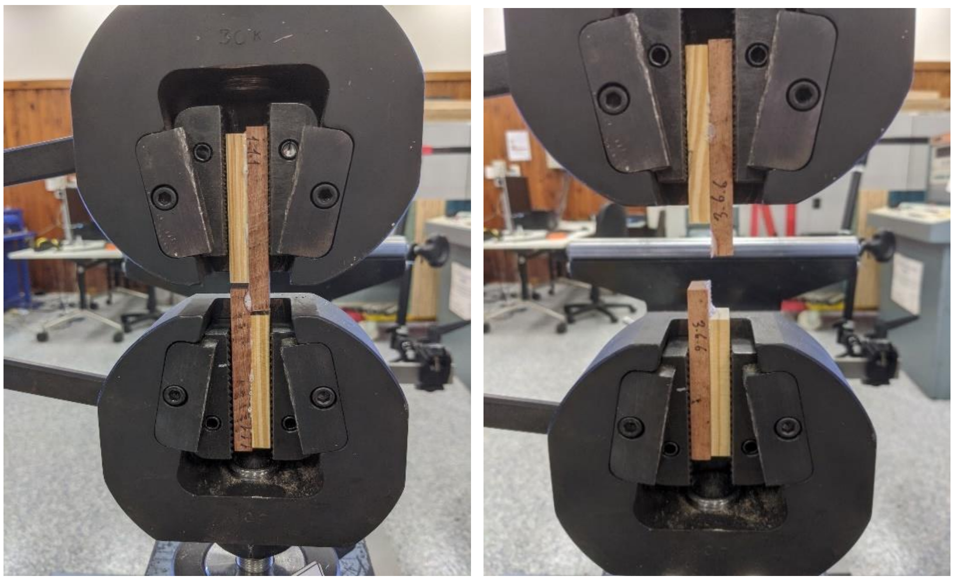

Fig. 6. Lap shear tensile strength testing

Statistical Analysis

Statistical analysis was carried out using GenStat v19 (VSN, Hemel Hempstead, United Kingdom). ANOVAs and pairwise comparisons using Fishers Protected Least Significant Differences testing were undertaken to compare treatment means when ANOVA showed significance in a factor. Because the different surface preparations, adhesive type and curing conditions were applied to sub-sections of the initial parent boards, it was appropriate to use randomized block analyses of the measured response variables with boards as blocks.

RESULTS AND DISCUSSION

Moisture Content

The mean moisture content of the boards prior to sample preparation and testing was 13%, with a range from 11% to 14%. These results are within the typical moisture content range of dried hardwood timber intended for milled products such as flooring and decking, and also compatible with expected moisture content targets for hardwood feedstock intended for glulam production.

Wettability

Across all surface machining treatments and timeframes after surface machining, the contact angle decreased over the 10-second test period from mean values above 60° to 22° for combined data (Table 3, Figs. 7 and 8). This reflects the typical wetting process, which includes: the formation of a contact angle between the surface and the droplet, the spreading of the droplet on the surface, and then the penetration of the droplet into the sample (Leggate *et al.* 2020a). The contact angle also tended to significantly increase and consequently surface wettability decrease with increasing time after surface machining ($p < 0.001$) (Fig. 9 and Table 3), with the exception of the planed surface machining treatment, which showed minimal change between timeframes post machining. For the face milling and sanding post-planing treatments, contact angles were lower (wettability higher) at 0 minutes compared to 15 minutes after surface machining (Table 3 and Figs. 7 and 8). This has been observed in other studies and has been attributed to 'ageing' of the wood surface linked to physical and chemical modifications of the wood surface (Gardner *et al*. 1991; Sernek 2002; Gindl *et al.* 2004; Piao *et al.* 2010*;* Santoni and Pizzo 2011; Qin *et al*. 2015; Leggate *et al.* 2020a). According to Burch (2015), a material's highest possible surface energy (therefore wettability) is obtained immediately following machining and exposure of a fresh surface. This reinforces the advantage of applying adhesive to the wood surface as soon as possible after surface machining.

When compared at the 10-second test time period, for both timeframes after surface machining, the highest mean contact angle and therefore the lowest surface wettability was recorded with the planing surface machining method (Table 3 and Figs. 7 and 8). For both 0 and 15 minutes after surface machining, face milling produced the lowest mean contact angle and therefore the highest surface wettability. The sanding post-planing also resulted in lower contact angles and higher wettability compared to planing. For 0 minutes after surface machining data, differences between the means for the three surface machining treatments were significantly different ($p < 0.01$), whereas for 15 minutes after surface machining, the planing had significantly lower wettability compared to face milling and sanding ($p < 0.01$). However, there were no significant differences between face milling and sanding. This result is comparable with studies on other species which report that the rougher surface produced by sanding or face milling improves the wettability of wood compared to planing (Stehr *et al.* 2001; Aydin 2004; Hernández and Cool 2008; Arnold 2010; Huang *et al.* 2012; Kläusler *et al.* 2014; Qin *et al.* 2015; Jankowska *et al.* 2018; Leggate *et al*. 2020a). Stehr *et al.* (2001) attributed the improved wettability of rougher surfaces to the increased surface area, which facilitates the movement and penetration of liquids due to capillary forces. Another explanation for the improved wettability with increased surface roughness is the greater exposure of hydrophilic active groups (hydroxyl groups) on the wood surface (Qin *et al.* 2015; Jankowska *et al.* 2018). The higher wettability of the face milling compared to the sanding post-planing may be due to the higher level of fibrillation that results from face milling. Fibrillation further increases the surface area which aids liquid wetting and penetration into the wood (Hernández and Cool 2008a).

The *K*-values shown in Table 3 represent the rate at which a liquid (in this case water) spreads and penetrates into the porous structure of wood (Huang *et al.* 2012; Leggate *et al*. 2020a). By knowing the *K*-value, spreading and penetration for a given liquid-solid system can be quantified and compared (Huang *et al.* 2012; Leggate *et al*. 2020a). Higher *K*-values indicate that the contact angle reaches equilibrium more rapidly and the liquid penetrates and spreads faster (increased wetting) (Huang *et al.* 2012). *K*-values are generally consistent with the contact angle data with, in most cases, lower *K*-values (therefore decreasing wettability of the surface) with increased time after surface machining. Lower *K*-values resulted with the planing treatment compared to the other surface machining methods. The highest *K*-values were produced with face milling. This result combined with achieving the lowest mean contact angle after the 10-second measurement period, indicates positive benefits of the face milling approach.

Table 3. Summary of Contact Angle Measurements

Surface Machining Method	Test Time (seconds)	Time after Surface Machining (minutes)	Mean Contact Angle (degrees)*	Mean *K*-value**
Planing	0	0	73 (8.4)	-
		15	72 (11.2)	-
	10	0	47 (6.0)	0.22
		15	47 (8.2)	0.20
Face Milling	0	0	70 (11.8)	-
		15	76 (13.2)	-
	10	0	22 (12.6)	0.40
		15	30 (10.3)	0.34
Sanding Post-Planing	0	0	62 (11.0)	-
		15	67 (14.0)	-
	10	0	29 (6.4)	0.31
		15	31 (9.6)	0.31

*Standard deviations are presented in parentheses
***K*-values are only calculated after 10 seconds, therefore not applicable to test time of 0 seconds

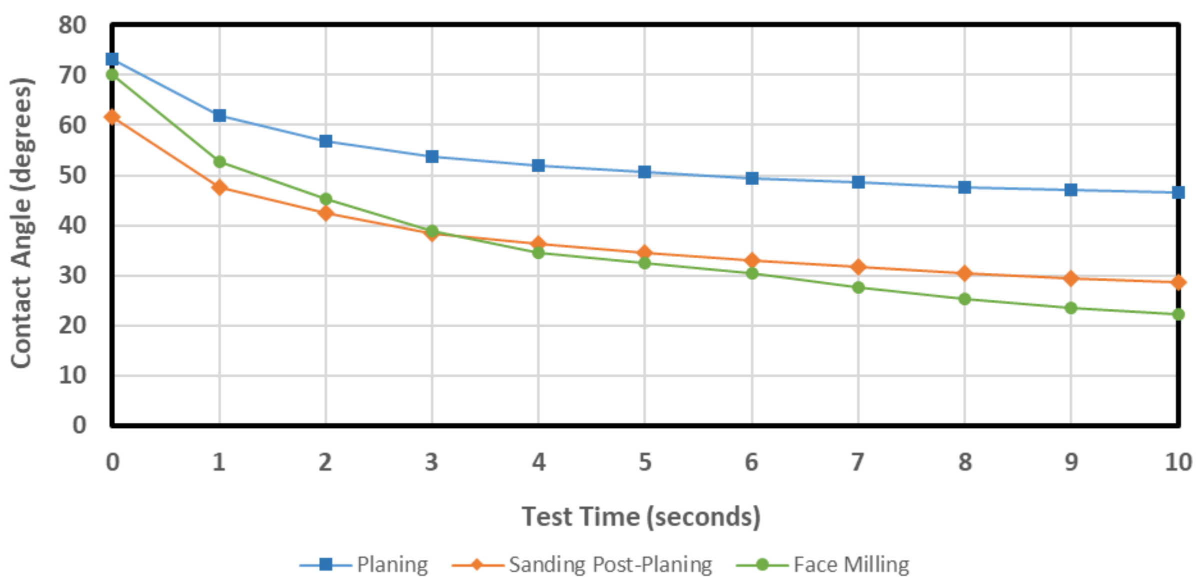

Fig. 7. Change in mean contact angle over a 10 second test time at 0 min after surface machining

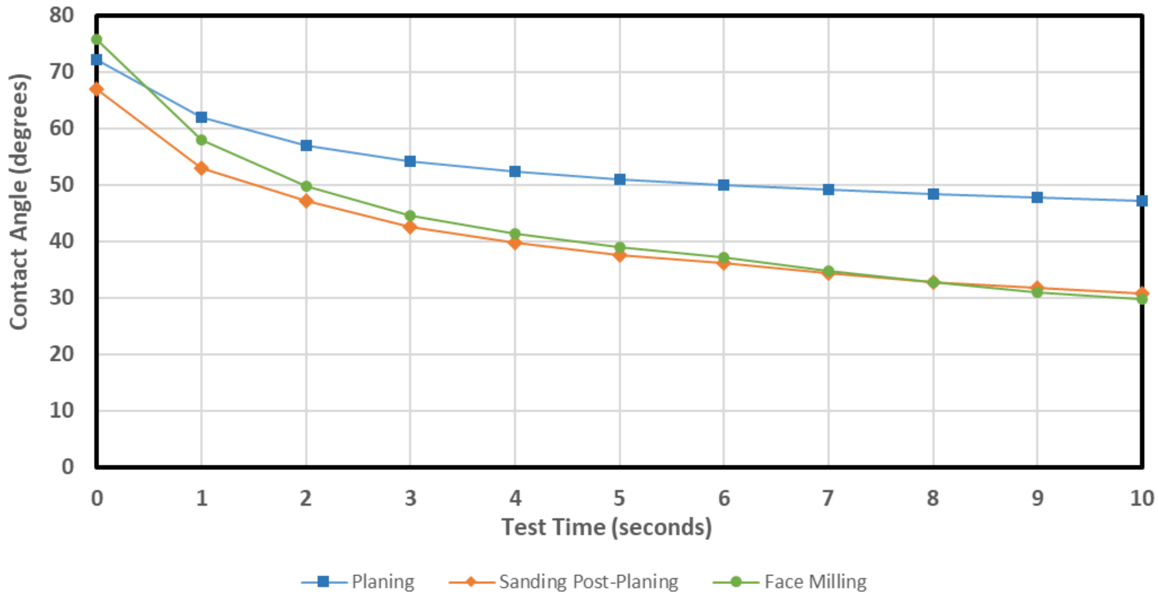

Fig. 8. Change in mean contact angle over a 10 second test time at 15 min after surface machining

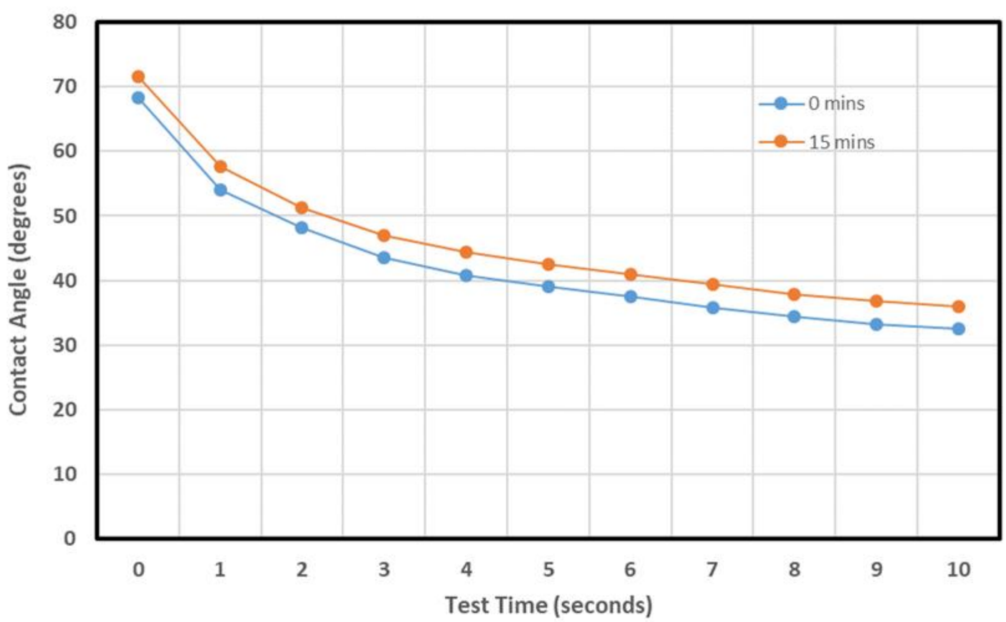

Fig. 9. Mean contact angle for different time intervals after surface machining and for each test time

Roughness

The planing resulted in significantly lower roughness (*i.e.* the smoothest surface) compared to face milling and sanding post-planing ($p < 0.01$); however, there were no significant differences in roughness between face milling and sanding post-planing (Table 4 and Fig. 10). While the effect of planing on roughness will usually vary with the planing equipment, planing configuration and blade sharpness (Knorz *et al.* 2015), this trend is consistent with other studies conducted on different species (*e.g.* De Moura *et al.* 2010; Kuljich *et al.* 2013; Zhong *et al.* 2013; Klausler *et al.* 2014; Kiliç 2015). Sanding post-planing and face milling produced similar surface roughness; however, sanding post-planing resulted in much lower variation indicating more homogeneity in the surface treatment (Fig. 10).

Higher wood surface roughness and fibrillation have been shown in other wood adhesion studies to: 1) increase the wood wettability, 2) improve the bonding strength through the facilitation of adhesive spreading by improved capillarity, 3) increase surface area for mechanical adhesion, and 4) increase the exposure of hydrophilic sites for the adhesive to bond to (Hernandez and Cool 2008a; Santoni and Pizzo 2011; Kläusler *et al.* 2014; Knorz *et al.* 2015; Qin *et al.* 2015; Jankowska *et al.* 2018; Leggate *et al.* 2020b). Fibrillation is also reported to improve wood adhesive bond performance by fortifying the adhesive layer and creating a more homogenous strain dissipation in the glue-line (Knorz *et al.* 2015; Leggate *et al.* 2020b).

Table 4. Summary of Roughness Assessments

Surface Machining Method	**Mean Ra** (µm)
Planing	9.73 (3.1) b
Sanding Post-Planing	14.34 (1.8) a
Face Milling	15.04 (5.2) a

Notes: Standard deviation shown in parenthesis; means followed by the same letter in the same column are not significantly different ($p < 0.01$)

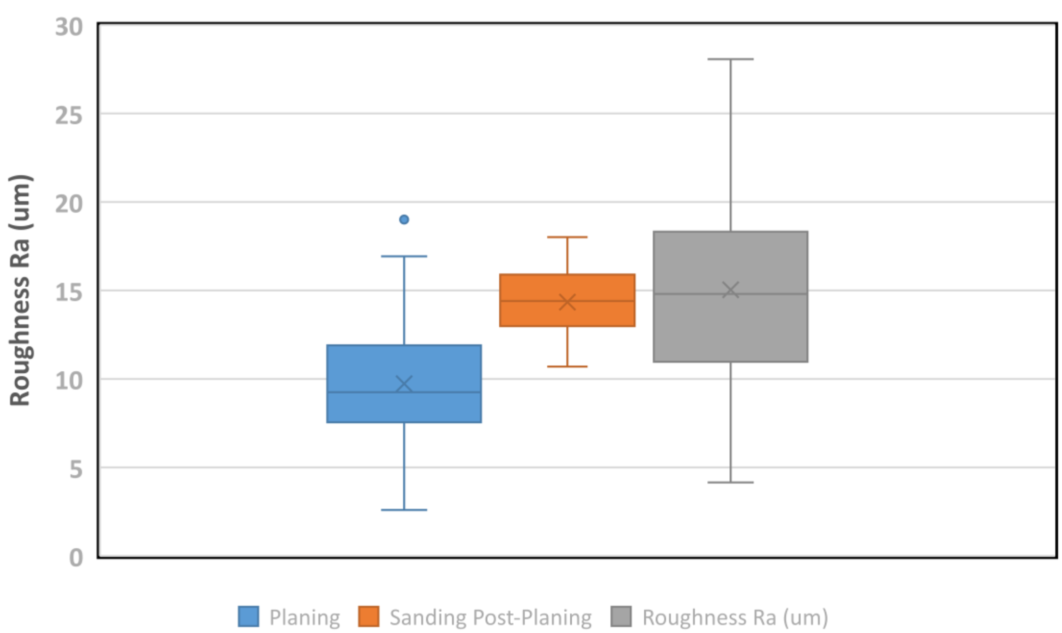

Fig. 10. Surface roughness (R_a) for each surface machining method

Permeability

Table 5 and Fig. 11 show the differences in gas permeability with each surface machining method. The highest permeability resulted from face milling, followed by sanding post-planing and then planing, which recorded the lowest permeability. There were significant differences between the means of the three surface machining treatments ($p<0.01$), as shown in Table 5. These results are consistent with the findings reported by Leggate *et al.* (2020a) for spotted gum sawn timber, where similar rankings for gas permeability were recorded. The differences in permeability between the three surface machining methods are likely to be attributed to the impact of these treatments on the surface topography and wood anatomy. The planing surface machining method is known to create more sub-surface damage and a less intact wood structure compared to face milling (Kläusler *et al.* 2014). This sub-surface damage includes cell compaction, crushing, and distortion, which may impede gas and liquid movement into the wood, potentially causing the lower permeability. The sanding post-planing would also be expected to have similar sub-surface damage as for planing; however, the sanding treatment will create a rougher surface, which may increase the surface area for gas and liquid penetration into the wood, possibly explaining the increased permeability compared to planing. The face milling method results in limited sub-surface damage plus the added advantages of increased fibrillation, which may improve permeability.

Further investigations of the influence of permeability on adhesive bond performance are warranted to better appreciate the interaction with other important adhesion parameters, such as glue penetration and glue line thickness. Investigating permeability at shallower depths from the surface may improve the understanding of wood permeability, adhesive penetration, and resulting bond performance. Additionally, microscopy and micro-computer tomography studies would also help explain the wood anatomical basis to permeability variation with different surface preparations.

Table 5. Summary of Permeability Results

Surface Machining Identifier	Mean Gas Permeability (mD)
Planing	3.82 (3.0) a
Face milling	34.06 (26.3) b
Sanding Post-Planing	17.42 (9.4) c

Notes: Standard deviation shown in parenthesis; means followed by the same letter in the same column are not significantly different ($p < 0.01$); *mD= millidarcies*

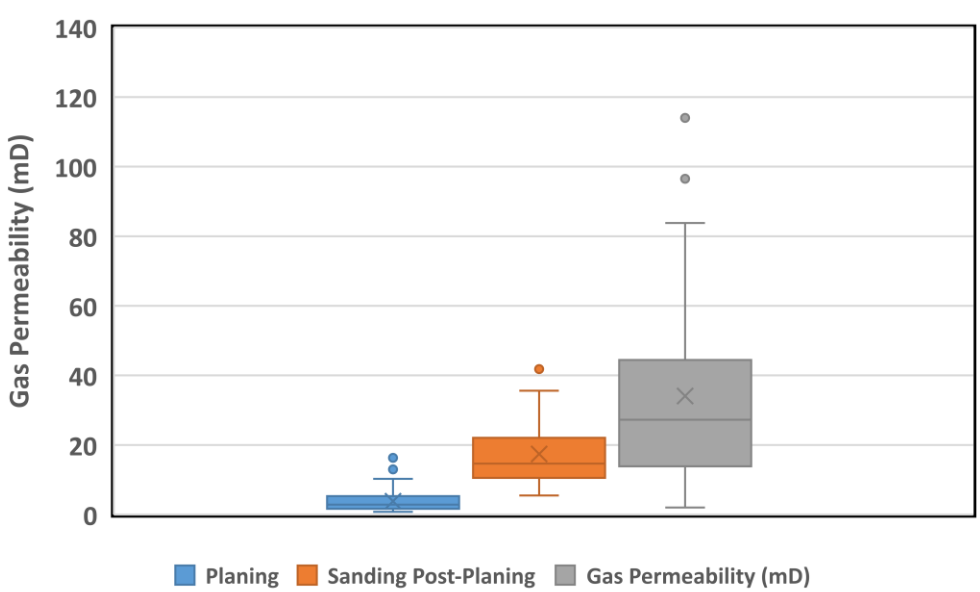

Fig. 11. Gas permeability for each surface machining method

Tensile Shear Strength

The lowest mean tensile shear strength for all adhesives and curing temperature scenarios resulted from the planing surface machining method (Table 6 and Fig. 12). With the exception of the Planing – RF Ambient Cure group, both face milling and sanding post-planing treatments resulted in significantly higher mean tensile shear strength compared to planing ($p < 0.01$) (Table 6).

Table 6. Summary of Tensile Shear Strength Results

Surface Machining Method	Adhesive Type and Curing Temperature	Mean Tensile Shear Strength (N/mm^2)
Planing	PUR - Ambient	11.44 (1.4) b
	RF - Ambient	12.87 (2.4) a
	RF – Elevated Temp.	9.58 (2.8) c
	Combined	11.30 (2.6) b
Face Milling	PUR - Ambient	12.93 (1.4) a
	RF - Ambient	13.05 (1.7) a
	RF – Elevated Temp.	13.65 (1.9) a
	Combined	13.21 (1.7) a
Sanding Post-Planing	PUR - Ambient	13.84 (1.4) a
	RF - Ambient	13.04 (2.5) a
	RF – Elevated Temp.	13.66 (1.9) a
	Combined	13.51 (2.0) a

Notes: Standard deviation shown in parenthesis; means followed by the same letter in the same column are not significantly different (0.01); N = newton

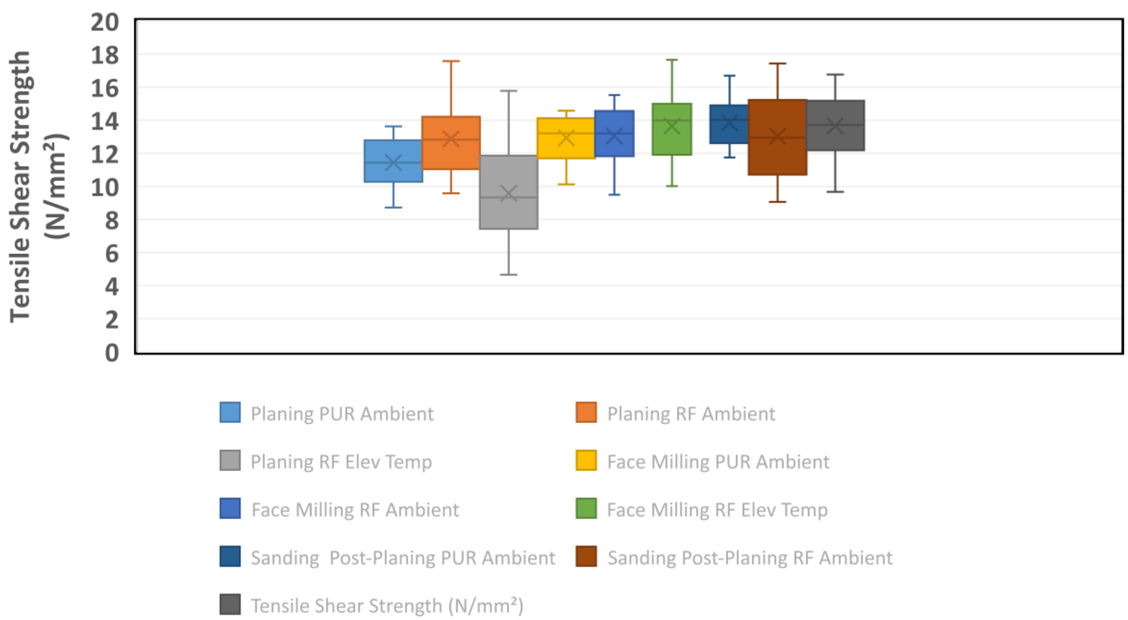

Fig. 12. Tensile shear strength for each surface machining method

The face milling and sanding post-planing surface machining methods produced similar results with no significant difference between them; however, sanding post-planing resulted in slightly higher mean tensile shear strength overall. Other studies have also reported better bond strength results with face milling or sanding compared to planing on different species (Knorz *et al.* 2015; Kuljich *et al.* 2013; Kläusler *et al.* 2014; Leggate *et al.* 2020b).

At ambient pressing temperatures, within each surface machining group, there was minimal difference in the tensile shear strength results between PUR and RF adhesives. However, the RF adhesive produced slightly higher mean tensile shear strength in all cases except for within the sanding post-planing group (Table 6 and Fig. 12). The elevated temperature curing of the RF adhesive resulted in slightly higher mean tensile shear strength for the face milling and sanding post-planing treatments compared to ambient temperature curing; however, the difference was not significant. Heating during curing of RF adhesives is thought to improve adhesive penetration and also support complete curing of the adhesive within the target press time. These factors may explain the slightly improved results using elevated temperature curing with the face milling and sanding post-planing groups. However, elevated temperature curing of the RF adhesive caused a significant reduction in the tensile shear strength for the planing surface machining treatment compared to ambient temperature curing. Further studies are needed to explain this result.

CONCLUSIONS

1. The pre-gluing surface machining method significantly influenced the roughness, wettability, permeability of Darwin stringybark timber, and tensile shear strength of bonded samples. Of the three surface machining methods trialed, planing resulted in the least rough (smoothest) surface (9.73 µm mean roughness), the lowest wettability (K value of 0.22 at 0 minutes after surface machining), and lowest gas permeability (3.82 mD). Samples bonded using this board preparation method also resulted in the lowest tensile shear strength (11.3 N/mm^2). This suggests that despite planing being the most common method adopted by industry internationally, using this method for preparing Darwin stringybark boards for bonding is likely to lead to poorer overall bond performance.
2. Face milling and sanding post-planing resulted in similar surface roughness (15.04 µm and 14.34 µm mean roughness respectively), wettability (K values of 0.40 and 0.31 respectively at 0 minutes after surface machining), and bonded samples performed similarly when tested for tensile shear strength (13.2 N/mm^2 and 13.5 N/mm^2 respectively). Face milling resulted in a significantly higher gas permeability than sanding post-planing (34.06 mD and 17.42 mD respectively).
3. Surface wettability significantly decreased with increasing time after surface machining. This reinforces the benefit of minimizing the time between surface machining and adhesive application.
4. At ambient pressing temperatures, within each surface machining treatment, there was minimal difference in the tensile shear strength between PUR and RF adhesives; however, the RF adhesive produced slightly higher mean tensile shear strength in all cases except for within the sanding post-planing group. This positive result supports ongoing inclusion of PUR adhesives in high density timber adhesion development activities. The elevated temperature curing of the RF adhesive resulted in slightly higher mean tensile shear strength for the face milling and sanding post-planing

treatments compared to ambient temperature curing; however, the difference was not significant. For the planing surface machining treatment, elevated temperature curing of the RF adhesive caused a significant reduction in the tensile shear strength compared to ambient temperature curing.

5. The results demonstrate that the choice of surface machining method prior to gluing is expected to influence the bond-performance results. For sawn timber-based EWPs manufactured from Darwin stringybark, face milling and sanding treatments post-planing provide better wood adhesion compared to planing. However, the full benefits of these alternative surface machining approaches may not be realized without optimizing the associated manufacturing protocols. For example, adjusting of manufacturing protocols (*e.g.* adhesive spread rates, open and closed assembly times, and press pressure conditions) with the selected board surface machining method will be necessary to ensure the improvements in potential bond performance can be realized.

ACKNOWLEDGMENTS

The authors are particularly grateful for the technical support of Mrs. Rica Minnett with the preparation, processing and testing of wood samples. Bob Mayer is thanked for his assistance with statistical analysis. The authors are also grateful to DTM Timber, in particular Mr. Curly Tatnell and Mr. Ian Haines, for the supply of the timber for this project. Mr. Shane Deveraux and Mr. Rod Vella from Jowat Universal Adhesives Australia Pty Ltd, and Mr. Scott Earnshaw and Mr. Alex Bruce from Hexion Pty Ltd are also thanked for the provision of the adhesives used in the study. The authors also especially acknowledge Mr. Mark Annandale and Dr. John Meadows from the University of the Sunshine Coast for their support along with providing funding from the Advance Queensland Innovation Program funded project 'Indigenous Employment, Forestry Livelihoods, Mining'. The support provided by the Queensland Government, Department of Agriculture and Fisheries (DAF) through the provision of the unique facilities located at the Salisbury Research Facility is acknowledged as critical to facilitate studies of this nature.

REFERENCES CITED

Arnold, M. (2010). "Planing and sanding of wood surfaces - Effects on surface properties and coating performance," in: *Proceedings PRA's 7th International Woodcoatings Congress*, Middlesex, Hampton, UK.

AS/NZS 1080.1 (2012). "Timber-Methods of test, Method 1: Moisture content," Standards Australia, Sydney, Australia.

AS 5604 (2005). "Timber – Natural durability ratings," Standards Australia, Sydney, Australia.

Aydin, İ. (2004). "Activation of wood surfaces for glue bonds by mechanical pre-treatment and its effects on some properties of veneer surfaces and plywood panels," *Applied Surface Science* 233(1-4), 268-274. DOI: 10.1016/j.apsusc.2004.03.230

Baty, F., Ritz, C., Charles, S., Brutsche, M., Flandrois, J. P., and Delignette-Muller, M.-L. (2015). "A toolbox for nonlinear regression in R: The package nlstools," *Journal*

of Statistical Software 66(5), 1-21.
BS EN 205 (2016). “Adhesives. Wood adhesives for non-structural applications. Determination of tensile shear strength of lap joints,” British Standards Institution, London, United Kingdom.
Burch, C. P. (2015). *Adhesion Fundamentals in Spotted Gum (Corymbia spp.)*, Master’s Thesis, Virginia Polytechnic Institute and State University, Blacksburg, VA, USA.
Butler, D. (2008). “Surface roughness measurement,” in: *Encyclopedia of Microfluids and Nanofluids*, D. Li (ed.), Springer, Boston, MA. DOI: 10.1007/978-0-387-48998-8_1506
CCOHS (2020). “Woodworking machines – Jointers and Planers,” (https://www.ccohs.ca/oshanswers/safety_haz/woodwork/planer.html), Canadian Centre for Occupational Health and Safety, Accessed 12 September 2020.
Comstock, G. L. (1968). *Physical and Structural Aspects of the Longitudinal Permeability of Wood*, Ph.D. Dissertation, State University of New York, Syracuse, NY, USA.
De Moura, L. F., Cool, J., and Hernàndez, R. E. (2010). “Anatomical evaluation of wood surfaces produced by oblique cutting and face milling,” *IAWA Journal* 31(1), 77-88. DOI: 10.1163/22941932-90000007
Fogg, P. J. (1968). *Longitudinal Air Permeability of Southern Pine Wood*, Ph.D. Dissertation, Louisiana State University, Baton Rouge, LA, USA.
Follrich, J., Vay, O., Veigel, S., and Müller, U. (2010). “Bond strength of end-grain joints and its dependence on surface roughness and adhesive spread,” *Journal of Wood Science* 56, 429-434. DOI: 10.1007/s10086-010-1118-1
Gardner, D. J., Generalla, N. C., Gunnells, D. W., and Wolcott, M. P. (1991). “Dynamic wettability of wood,” *Langmuir* 7(11), 2498-2502.
Gindl, M., Reiterer, A., Sinn, G., and Stanzl-Tschegg, S. E. (2004). “Effects of surface ageing on wettability, surface chemistry and adhesion of wood,” *Holz Als Roh-und Werkstoff* 62(4),273-280. DOI: 10.1007/s00107-004-0471-4.
Gooch, J. W. (2011). “Tensile-shear strength,” in: *Encyclopedic Dictionary of Polymers*, J.W. Gooch (ed.), Springer, New York, NY. DOI: 10.1007/978-1-4419-6247-8-_11631
Hansmann, C., Gindl, W., Wimmer, R., and Teischinger, A. (2002). “Permeability of wood – A review,” *Wood Research* 47(4), 1-16.
Hernández, R. E., and Cool, J. (2008a). “Effects of cutting parameters on surface quality of paper birch wood machined across the grain with two planing techniques,” *Holz als Roh - und Werkstoff* 66, 147-154. DOI: 10.1007/s00107-007-0222-4
Hernández, R. E., and Cool, J. (2008b). “Evaluation of three surfacing methods on paper birch wood in relation to water and solvent-borne coating performance,” *Wood Fiber Science* 40(3), 459-469.
Hovanec, D. (2015). *Effect of Wood Characteristics on Adhesive Bond Quality of Yellow-Poplar for Use in Cross-laminated Timbers*, Master’s Thesis, West Virginia University, Morgantown, WV, USA.
Huang, I., Kocaefe, D., Boluk, Y., Kocaefe, Y., and Pichette, A. (2012). “Effect of surface preparation on the wettability of heat-treated jack pine wood surface by different liquids,” *European Journal Wood Products* 70, 711-717. DOI: 10.1007s00107-012-0605-z.
ISO 4287 (1997). “Geometrical Product Specifications (GPS) – Surface texture: Profile method – Terms, definitions and surface texture parameters,” International

Organization for Standardization (ISO), Geneva, Switzerland.
Jankowska, A., Zbiec, M., Kozakiewicz, P., Koczan, G., Olenska, S., and Beer, P. (2018). "The wettability and surface free energy of sawn, sliced and sanded European oak wood," *Maderas. Ciencia y Technologia* 20(3), 443-454. DOI: 10.4067/S0718-221X2018005031401
Kiliç, M., (2015). "Effects of machining methods on the surface roughness value of *Pinus nigra* Arnold wood," *BioResources* 10(3), 5554-5560. DOI: 10.15376/biores.10.3.5554-5562
Kläusler, O., Rehm, K., Elstermann, F., and Niemz, P. (2014). "Influence of wood machining on tensile shear strength and wood failure percentage of one-component polyurethane bonded wooden joints after wetting," *International Wood Products Journal* 5(1), 18-26. DOI: 10.1179/204264531Y.0000000039
Knorz, M., Neuhaeuser, E., Torno, S., and Van de Kuilen, J. W. (2015). "Influence of surface preparation methods on moisture-related performance of structural hardwood-adhesive bonds," *International Journal of Adhesion and Adhesives* 57(2015), 40-48. DOI: 10.1016/j.ijadhadh.2014.10.003
Kucerová, I. (2012). "Methods to measure the penetration of consolidant solutions into dry wood," *Journal of Cultural Heritage* 2012(13), 191-195. DOI: 10.1016/j.culher.2012.04.012.
Kuljich, S., Cool, J., and Hernández, R. E. (2013). "Evaluation of two surfacing methods on black spruce wood in relation to gluing performance," *Journal of Wood Science* 59, 185-194. DOI: 10.1007/s10086-012-1318-y
Kumar, R. N., and Pizzi, A. (2019). *Adhesives for Wood and Lignocellulosic Materials*, John Wiley & Sons Inc., Hoboken, NJ, USA.
Lamour, G., Hamraoui, A., Buvailo, A., Xing, Y., Keuleyan, S., Prakash, V., Eftekhari-Bafrooei, A., and Borguet, E. (2010). "Contact angle measurement using a simplified experimental setup," *Journal of Chemical Education* 87(12), 1403-1407. DOI: 10.1021/ed100468u
Ledinek (2020). "Rotoles revolution," (https://www.ledinek.com/rotoles-d), Accessed 12 September 2020.
Leggate, W. (2018). *Improving the Durability Performance of Engineered Wood Products: A Study Tour of Europe and North America* (Gottstein Fellowship Report), Gottstein Trust, Melbourne, Australia.
Leggate, W., Redman, A., Wood, J., Bailleres, H., and Lee, D.J. (2019). "Radial permeability of the hybrid pine (*Pinus elliottii* x *Pinus carbaea*) in Australia," *BioResources* 14(2), 4358-4372. DOI: 10.15376/biores.14.2.4358-4372.
Leggate, W., McGavin, R., Miao, C., Outhwaite, A, Chandra, K., Dorries, J., Kumar, C., and Knackstedt, M. (2020a). "The influence of mechanical surface preparation methods on southern pine and spotted gum wood properties: Wettability and Permeability," *BioResources* 15(4), 8554-8576. DOI: 10.15376/biores.15.4.8554-8576.
Leggate, W., McGavin, R., Outhwaite, A., Kumar, C., Faircloth, A., and Knackstedt, M. (2020b). "The influence of mechanical surface preparation methods on the bonding of southern pine and spotted gum: tensile shear strength of lap joints," *BioResources* In Press.
Lehringer, C., and Gabriel, J. (2014). "Review of recent research activities on one-component PUR-adhesives for engineered wood products," in: *Materials and Joints in Timber Structures*, S. Aicher, H. W. Reinhardt, and H. Garrecht (eds.), Springer,

Dordrecht, Netherlands, pp. 405-420. DOI:10.1007/978-94-007-7811-537
Market Research Future (2020). "Engineered wood market research report – forecast to 2023," (https://www.marketresearchfuture.com/reports/engineered-wood-market-4791), Accessed 24 July 2020.
Milota, M., Tschernitz, J. L., Verrill, S. P., and Mianowski, T. (1994). "Gas permeability of plantation loblolly pine," *Wood and Fiber Science* 27(1), 34-40.
Piao, C., Winandy, J. E., and Shupe, T. F. (2010). "From hydrophilicity to hydrophobicity: A critical review. Part 1. Wettability and surface behaviour," *Wood & Fiber Science* 42(4), 490-510.
Qin, Z., Zhang, Q., Gao, Q., Zhang, S., and Li, J. (2015). "Wettability of sanded and aged fast-growing poplar wood surfaces: I. Surface free energy," *BioResources* 9(4), 7176-7188. DOI: 10.15376/biores.9.4.7176-7188
River, B. H., Vick, C. B., and Gillespie, R. H. (1991). *Wood as an Adherend*, New York. Marcel Dekker.
RStudio Team (2015). RStudio: Integrated development for R. RStudio, Inc, Boston, MA URL http://www rstudio com 42:14
Santoni, I., and Pizzo, B. (2011). "Effect of surface conditions related to machining and air exposure on wettability of different Mediterranean wood species," *International Journal of Adhesion and Adhesives* 31(7), 743-753. DOI: 10.1016/j.ijadhadh.2011.07.002
Schneider, C. A., Rasband, W. S., and Eliceiri, K. W. (2012). "NIH Image to ImageJ: 25 years of image analysis," *Nature Methods* 9(7), 671-675, PMID 22930834. DOI: 10.1038/nmeth.2089.
Shi, S. Q., and Gardner, D. J. (2001). "Dynamic adhesive wettability of wood," *Wood and Fiber Science* 33(1), 58-68.
Sernek, M. (2002). *Comparative Analysis of Inactivated Wood Surfaces*, Ph.D. Dissertation, Faculty of the Virginia Polytechnic Institute and State University, Blacksburg, VA, USA.
Stehr, M., Gardner, D. J., and Walinder, M. E. P. (2001). "Dynamic wettability of different machined wood surfaces," *Journal of Adhesion* 76(3), 185-200. DOI: 10.1080/00218460108029625.
Tesoro, F. O. (1973). *Factors Affecting the Flow of Gas and Liquid through Softwoods and Hardwoods*, Ph.D. Dissertation, Louisiana State University, Baton Rouge, LA, USA.
Vella, R., Heitzmann, M. T., and Redman, A. (2019). "Improving the adhesion of high-density softwoods with isocyanate based adhesives through surface incision," *BioResources* 14(4), 7751-7762. DOI: 10.15376/biores.14.4.7751-7762
Vella, R. (2020). *Improving the Adhesion of High-density Softwoods with Isocyanate Based Adhesives*, Master's Thesis, University of Queensland, Brisbane, QLD, Australia.
Vick, C. B. (1999). "Adhesive bonding of wood materials," in: *Wood Handbook: Wood as an Engineering Material*, USDA Forest Service, Forest Products Laboratory, Madison, WI, USA.
Wellons, J. D. (1980). "Wettability and gluability of Douglas-fir veneer," *Forest Products Journal* 30, 53-55.
Zhong, Z. W., Hiziroglu, S., and Chan, C. T. M. (2013), "Measurement of the surface roughness of wood-based materials used in furniture manufacture," *Measurement* 46, 1482-1487. DOI: 10.1016/j.measurement.2012.11.041

Zimmer, K. P., Høibø, O. A., Vestøl, G. I., and Larnøy, E. (2014). "Variation in treatability of Scots pine sapwood: A survey of 25 different northern European locations," *Wood Science and Technology* 48(5), 1049-1068. DOI: 10.1007/s00226-014-0660-1.

Zisman, W. A. (1964). "Relation of the equilibrium contact angle to liquid and solid Constitution," in: *Contact Angle, Wettability and Adhesion*, American Chemical Society, Washington, D.C. DOI: 10.1021/ba-1964-0043.ch001

Article submitted: September 20, 2020; Peer review completed: October 18, 2020; Revised version received and accepted: November 3, 2020; Published: November 16, 2020.

DOI: 10.15376/biores.16.1.302-323